
GQA- μ P: THE MAXIMAL PARAMETERIZATION UPDATE FOR GROUPED QUERY ATTENTION

Kyle R. Chickering* **Huijuan Wang*** **Mengxi Wu*** **Alexander Moreno**
 UC Davis & MBZUAI IFM USC & MBZUAI IFM USC MBZUAI IFM

Muhao Chen **Xuezhe Ma** **Daria Soboleva** **Joel Hestness**
 UC Davis USC & MBZUAI IFM Cerebras Cerebras

Zhengzhong Liu **Eric Xing**
 MBZUAI IFM Carnegie Mellon University & MBZUAI IFM

ABSTRACT

Hyperparameter transfer across model architectures dramatically reduces the amount of compute necessary for tuning large language models (LLMs). The maximal update parameterization (μ P) ensures transfer through principled mathematical analysis but can be challenging to derive for new model architectures. Building on the spectral feature-learning view of Yang et al. (2023a), we make two advances. First, we promote spectral norm conditions on the weights from a heuristic to the definition of feature learning, and as a consequence arrive at the Complete-P depth and weight-decay scalings without recourse to lazy-learning. Second, we consider a modified spectral norm that preserves the valid scaling law of network weights when weight matrices are not full rank. This enables (to our knowledge, the first) derivation of μ P scalings for grouped-query attention (GQA). We demonstrate the efficacy of our theoretical derivations by showing learning rate transfer across the GQA repetition hyperparameter as well as experiments regarding transfer over weight decay.

1 INTRODUCTION

The maximal update parametrization (μ P) (Yang & Hu, 2021; Yang et al., 2022) provides principled rules for zero-shot learning rate transfer across model widths. Thus, large terminal model hyperparameters can be determined by sweeping a small proxy model. μ P has been used to train models up to at least 13B parameters with zero-shot transfer (Blake et al., 2023; Dey et al., 2023; Narayan et al., 2025). Its applicability, however, has been largely limited to learning rate transfer across model widths. To broaden this scope, Dey et al. (2025) introduced Complete-P, extending the original prescriptions to weight decay and model depth. However, many common architectures that are widely deployed in production still lack established μ P scalings.

This paper seeks to close this gap by extending the spectral μ P framework of Yang et al. (2023a) to be more practically useful in deriving μ P prescriptions for novel architectures. As an example of the utility of our framework, we derive (to our knowledge, the first) μ P scaling for grouped-query attention (GQA) (Ainslie et al., 2023). Our analysis reveals that GQA surfaces several difficulties that prior work has left unaddressed. First, when using GQA the original μ P implementation passes coordinate checks, i.e., the customary correctness tests for the implementation. However, empirical analysis shows that the original μ P implementation fails to transfer learning rates, seemingly contradicting established theory (see Figures 1 and 5). We resolve this by extending the spectral-norm version of μ P introduced in Yang et al. (2023a), and showing that the original μ P implementation does not pass a more rigorous spectral-norm coordinate check. Second, the intrinsic low rank of

*Equal contribution

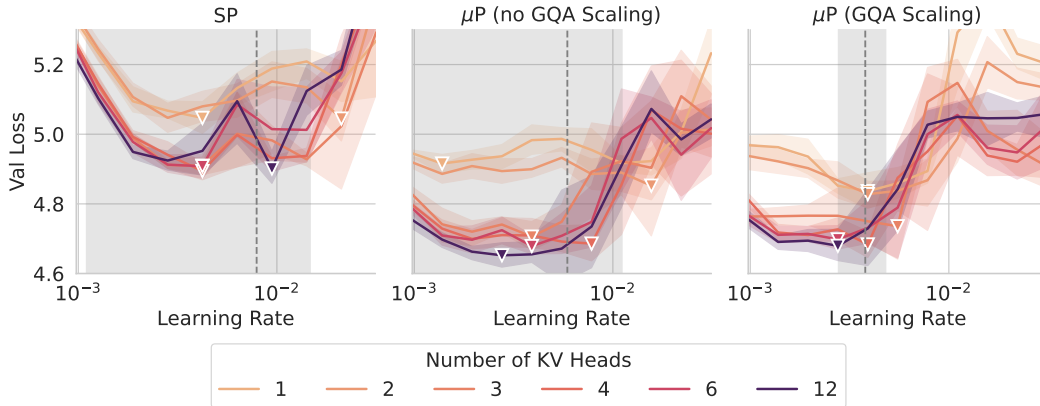


Figure 1: Comparison of the standard parameterization (left), the vanilla Adam- μP parameterization (middle), and our GQA- μP scaling (right). For a fixed model size, we vary the number of KV heads. The dashed lines indicate the mean optimal learning rates for each parameterization, and the shaded grey region denotes the standard deviation of the optimal learning rates. All models are trained to 10 tokens per parameter (TPP). Additional details can be found in Appendix B.1.2.

GQA weight matrices skews the expected size of layer outputs. To address this issue, we introduce a new norm, namely the expected operator norm, to replace the spectral norm in spectral μP theory and restore the desired scaling behavior.

Our primary contributions are threefold:

1. We extend the spectral μP theory of Yang et al. (2023a), which allows derivations of μP for more advanced architectures like weight decay, recursion blocks, and GQA. Our work provides, to our knowledge, the first derivation of μP scaling for GQA.
2. We perform empirical analysis to validate the theory and offer practical guidance for learning rate transfer across GQA settings. In particular, we suggest that transferring across different numbers of GQA repetitions leads to noisy transfer dynamics, suggesting caution when attempting to transfer learning rate.
3. Our experiments show that, with the correct scalings, both weight decay and the training-time constant τ_{epoch} introduced in Wang & Aitchison (2024) appear to be transferable.

2 RELATED WORK

Foundations of μP : μP builds on a series of works by Yang, developing the Tensor Programs framework (Yang, 2019; 2020a;b; Yang & Hu, 2021; Yang et al., 2022; 2023b). This line of work uses random matrix theory to carefully analyze the mathematical properties of neural networks during training, while also empirically demonstrating that these theoretical approaches remain valuable for real-world deep learning. Within the framework of Tensor Programs, Yang et al. (2022) derives the well-known μP scaling laws for width under SGD and Adam training. The final paper in the series Yang et al. (2023b) attempts to extend μP to depth scalings. However, they were unable to extend to the case of residual blocks with standard configurations for the hidden layers. Finally, the foundation of the mathematical framework presented in this work builds on Yang et al. (2023a), who show an alternative derivation of the results in Yang et al. (2022) based on spectral norms.

Models using GQA: Group-query attention (GQA) (Ainslie et al., 2023) is an efficient attention mechanism that reduces memory usage by sharing key and value heads across groups of query heads. Due to its favorable trade-off between memory efficiency and model performance, GQA has been widely used in modern large language models, including Mistral 7B (Jiang et al., 2023), LLaMA 3 (Grattafiori et al., 2024), Qwen3 (Yang et al., 2025) and K2-V2 (Liu et al., 2025).

Extensions of μP : The original μP formulation presented in Yang et al. (2022) applies only to scaling the width of a fixed depth, fixed batch size neural network. While already a powerful tool, later

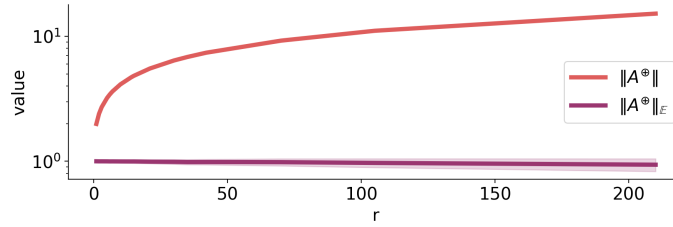


Figure 2: Demonstration of the failure of the spectral norm to accurately capture the behavior for low-rank matrices when the inputs are randomly sampled i.i.d. from $\mathcal{N}(0, 1)$. r is the number of key-value head repetitions and $r = 1$ corresponds to the setting without GQA. Each point is averaged over 1000 independent draws of \mathbf{A} , with the shaded band showing ± 1 standard deviation.

authors have sought to extend the principles of μP to cover cases not covered by the original formulation. Dey et al. (2023) do large-scale validation experiments using μP and find empirical evidence that learning rate can transfer across batch and dataset size. Dey et al. (2023) suggests μP -type scalings for weight decay, the Adam ε , and depth. Their contributions to depth scaling are most notable, as their empirical findings contradict the scaling presented in Yang et al. (2023b). However, their extensive empirical analysis suggests that the scaling they derive is correct. We arrive at the same scaling in Section 3.3 using the framework we outline in this paper. More recently Mlodozieniec et al. (2025) extended the work of Dey et al. Dey et al. (2025) by extending the SDE parameterization to cover hyperparameter transfer for batch size, as well as showing the value of per-layer learning rate tuning.

Blake et al. (2023) apply μP in the context of large-scale, low-precision LLM training. They use ABC parameterizations to apply the μP scaling rules while maintaining unit variance for all layers in the network, which they refer to as unit scaling- μP . Additionally, they empirically validate that learning rate transfer persists across datasets, batch sizes, depths, and training iterations under controlled conditions. Narayan et al. (2025) suggest a different, more simplified version of the unit scaling- μP which they also show works for training low-precision networks with μP .

Finally, a related subsequent work Zheng et al. (2026) has proposed a similar theoretical framework to ours. Both our work and theirs share the perspective that the spectral norm provides a principled alternative to Tensor Programs Yang & Hu (2021) for deriving μP . However our works differ in scope and motivation. Zheng et al. (2026) systematically apply their framework to a broad class of optimizers under width and depth scaling, while our work identifies the expected operator norm as necessary to correctly handle rank-degenerate weights and using this norm to provide the first derivation of μP for GQA.

3 DERIVING NOVEL MAXIMAL UPDATE PARAMETERIZATIONS

Consider a collection of weight matrices $\mathbf{W}^\ell \in \mathbb{R}^{n_\ell \times m_\ell}$ in a neural network, indexed by layer ℓ . Yang et al. (2023a) proves that conditions imposed upon the weight matrices of a network imply feature learning (and thus learning rate transfer) as defined in Yang et al. (2022) (see Equation 3). For initial weights \mathbf{W}_0^ℓ and iterates $\mathbf{W}_t^\ell = \mathbf{W}_0^\ell + \sum_{k=1}^t \Delta \mathbf{W}_k^\ell$, where $\Delta \mathbf{W}_t^\ell = \mathbf{W}_t^\ell - \mathbf{W}_{t-1}^\ell$, Yang et al. (2023a) suggests that both the initialization and the updates must satisfy:

$$\|\mathbf{W}_0^\ell\| = \Theta(\sqrt{n_\ell}/\sqrt{m_\ell}), \quad \|\Delta \mathbf{W}_t^\ell\| = \Theta(\sqrt{n_\ell}/\sqrt{m_\ell}), \quad (1)$$

where $\|\mathbf{W}\| := \sup_{\|x\|_2=1} \|\mathbf{W}x\|_2$ is the usual spectral (or induced) norm. This spectral perspective on feature learning is powerful, and we introduce three minor but important modifications that enable us to extend the method of Yang et al. (2023a) to cover novel architectures like GQA.

Analysis Under a New Norm: The spectral norm can be interpreted as the maximal deformation of an input vector induced by an operator $\varphi : \mathbb{R}^m \rightarrow \mathbb{R}^n$. For full-rank operators, such as dense feed-forward layers, random matrix theory shows that the quantitative value of the spectral norm is attained asymptotically. In the classical case of an $n \times n$ random matrix A , we have the sharp asymptotic relation $\|A\| = 2\sqrt{n}$ as $n \rightarrow \infty$.

However, for rank-degenerate matrices like those used in GQA, the spectral norm is not attained asymptotically in practice. The reason is that, as shown by Tensor Programs Yang & Hu (2021), the inputs to a GQA layer during training are i.i.d., and therefore, for rank-degenerate matrices, the vectors that cause this “maximal deformation” occur with probability zero! A visualization of this discrepancy can be seen in Figure 2. Instead, we should use a notion of size that reflects the actual deformation encountered during training.

To this end, let Ω be the probability distribution of the input vectors. We define the **expectation operator norm** as¹

$$\|A\|_{\mathbb{E},\Omega,p} := \mathbb{E}_{x \sim \Omega} \left[\frac{\|Ax\|_p}{\|x\|_p} \right]. \quad (2)$$

Throughout this paper, we adopt the convention $\|A\|_E = \|A\|_{\mathbb{E},\mathcal{N}(0,1),2}$, where $x \sim \mathcal{N}(0,1)$ has i.i.d. entries. Crucially, when A is square with i.i.d. entries, it has full rank with probability one, and we obtain the asymptotic relationship $\|A\|_{\mathbb{E}} = \Theta(\|A\|)$. A proof is provided in Lemma 2.

Operator-Norm Focused Feature Learning: Yang et al. (2023a) shows that constraining the spectral norm of the weight matrices implies feature learning in the sense of Yang & Hu (2021), where feature learning is defined to occur when

$$\|h_0^\ell\|_2 = \Theta(\sqrt{n}), \quad \|\Delta h_t^\ell\|_2 = \Theta(\sqrt{n}), \quad (3)$$

for all pre-activations h^ℓ . In particular, Yang et al. (2023a) prove that enforcing condition equation 1 on spectral norms implies equation 3. However, the converse does not hold: feature learning in the sense of equation 3 may still occur even if the weight matrices do not scale according to equation 1.

Consider a hidden layer $h(x) = \mathbf{W}x$ with trainable weights $\mathbf{W} \in \mathbb{R}^{n \times n}$ and an additional scaling parameter, the number of layers $L > 1$ independent of n , for which we want to ensure feature learning as $L \rightarrow \infty$. Under proper initialization, i.e. $\|\mathbf{W}_0\| = \Theta(1)$, we have $\|h(x)\|_2 = \Theta(\sqrt{n})$ for $x \in \mathbb{R}^n$ with $\|x\|_2 = \Theta(\sqrt{n})$, as required by feature learning. Now suppose the learning rate is set incorrectly, and $\|\Delta \mathbf{W}_t\| = \Theta(L^{-\alpha})$ for some $0 < \alpha$. Then the weight update takes the form

$$\Delta h_t = \mathbf{W}_t x_t - \mathbf{W}_{t-1} x_{t-1} = \Delta \mathbf{W}_t x_t + \mathbf{W}_{t-1} \Delta x_t.$$

Assuming that these terms do not exactly cancel, and noting that $\|\Delta x_t\|_2 = \Theta(\sqrt{n})$, we have that

$$\|\Delta h_t\| = \Theta(\sqrt{n}(1 + L^{-\alpha})) = \Theta(\sqrt{n}),$$

and thus this layer satisfies feature learning in the sense of equation 3. For GQA, this precise situation arises, and the subtle failure of the terms Δh_t to properly scale leads to a failure of learning rate transfer (see Figures 5 and 1 below).

This analysis shows that the spectral condition of equation 1 is a stronger notion of feature learning than equation 3 and we propose using it as the **definition** of feature learning. This perspective has beneficial practical consequences. When doing coordinate checking to validate a μP implementation as shown in (Yang et al., 2022), we found that directly analyzing the weight matrices proves more effective than analyzing only the activations (see Figure 4). This point is discussed further below.

A Functional Analytic View of Layer-Wise Computation: Modern machine learning architectures consist of more than dense feed-forward units. Thus, we propose focusing on the computational units of the network rather than specifically focusing on matrices. In the case of dense feed-forward layers, these notions coincide. But for residual layers our perspective offers a more unifying approach. Concretely, we regard a neural network not only as a compositional sequence of matrix multiplications, but as a compositional sequence of abstract, generally non-linear mappings $\varphi^\ell : \mathbb{R}^m \rightarrow \mathbb{R}^n$.

We suggest that the first part of the spectral condition in equation 1 should be applied to each compositional unit, rather than the matrices themselves. Starting with the end-to-end computation of the network, we recursively apply this condition to all mappings φ^ℓ . In conjunction with requiring that all trainable parameters satisfy both parts of equation 1, this leads to a unified treatment of residual layers which we discuss below.

¹Technically, the object we define as $\|A\|_{\mathbb{E},\Omega,p}$ is only a seminorm without further constraints on Ω . In particular, if $\text{supp } \Omega \neq \mathbb{R}^n$ then it is possible for all random vectors $x \sim \Omega$ to lie in the nullspace of A . This edge case does not occur in neural network training.

Table 1: The table summarizes the parameterization of Transformers with Grouped-Query Attention (GQA), where n denotes the input dimension and r is the number of key-value head repetitions. Modifications specific to GQA are highlighted in blue. The derivations of learning rate and weight decay follow the AdamW implementation in PyTorch.

	Embed.	Unemb.	Attn. (Q, O)	Attn. (K, V)	Feed-forward
Init. Var.	1	1	$1/\sqrt{n}$	$1/\sqrt{n}$	$1/\sqrt{n}$
Multiplier	1	$1/n$	1	1	1
LR	1	1	$1/n$	$(1 + \sqrt{r})/(2n)$	$1/n$
Weight Decay	1	1	n	$2n/(1 + \sqrt{r})$	n

3.1 WEIGHT DECAY

Weight decay is commonly applied in deep learning to stabilize model training dynamics (Loshchilov & Hutter, 2017; Andriushchenko et al., 2023). For concreteness, we focus on AdamW (Loshchilov & Hutter, 2017) in this section, although our framework extends well to other optimizers, such as MuON (Jordan et al., 2024), with weight decay. AdamW modifies the Adam weight update equation 12 by including a weight decay term with the associated weight decay hyperparameter²

We begin by defining the update rule for AdamW. The total parameter update $\Delta \mathbf{W}_t$ is composed of two distinct terms: a weight decay term and the standard Adam gradient-based update $\hat{\mathbf{r}}_t$:

$$\Delta \mathbf{W}_t = -\lambda \eta \mathbf{W}_t - \eta \hat{\mathbf{r}}_t. \quad (4)$$

For the learning dynamics to remain consistent (transferable) as we scale the network width n , the spectral norms of these two contributions must scale identically. Specifically, the weight decay magnitude must match the gradient update magnitude, and both must remain stable relative to the weights themselves. Mathematically, this balance condition is expressed as:

$$\|\Delta \mathbf{W}_t\| = \Theta(\lambda \eta \|\mathbf{W}_t\|) = \Theta(\eta \|\mathbf{r}_t\|) = \Theta(1).$$

Given that $\|\Delta \mathbf{W}_t\| \approx \|\mathbf{W}_t\|$ in the feature learning limit, it follows that the weight decay coefficient must satisfy $\lambda \eta = \Theta(1)$. Recall that μP prescribes specific learning rates η depending on the layer type: $\eta = \Theta(1)$ for input layers, and $\eta = \Theta(1/n)$ for hidden and output layers. To maintain the balance described above, the base weight decay λ_0 must be scaled as follows. For input Layers, since $\eta = \Theta(1)$, we require $\lambda^0 = \Theta(1)$. For the hidden and output Layers, since $\eta = \Theta(1/n)$, we require $\lambda^\ell = \Theta(n)$.

Let us analyze the dynamics of a hidden layer where we introduce a scaling error $\delta > 0$. Suppose we set $\lambda^\ell = \lambda_0 n^{1+\delta}$. To maintain a stable update size, the learning rate needs to compensate, scaling as $\eta = \Theta(n^{-1-\delta})$. As $n \rightarrow \infty$, $\eta \hat{\mathbf{r}}_t$ becomes negligible. The weight decay term dominates $\Delta \mathbf{W}_t \approx -\eta_0 \lambda_0 \mathbf{W}_t$. Consequently, the model ignores the data entirely, and the weights simply decay toward $\mathbf{0}$ without learning features. Conversely, suppose we set $\lambda = \lambda_0 n^{1-\delta}$. This implies standard μP learning rate $\eta = \Theta(n^{-1})$ is relatively larger compared to the decay strength. As $n \rightarrow \infty$, $\Delta \mathbf{W}_t \approx -\eta \hat{\mathbf{r}}_t$ vanishes. The weight decay is effectively ignored. The algorithm collapses back to standard Adam, losing the regularization benefits of AdamW. Thus, the scaling $\lambda = \Theta(n)$ maintains the necessary equilibrium between regularization and feature learning at large widths.

Recent studies by Wang & Aitchison (2024) and Dey et al. (2025) have derived a similar relation between learning rate and weight decay through different methods. We experimentally validate this relationship in Figure 7.

²We focus on **coupled** weight decay, which is the type of weight decay included in PyTorch (Schaipp, 2024). However, the weight decay introduced in Loshchilov & Hutter (2017) is **decoupled** and given by $\Delta \mathbf{W}_t = -\lambda \mathbf{W}_t - \eta \hat{\mathbf{r}}_t$. Our results still apply in this case and prescribe the scaling $\lambda = \lambda_0$, where λ_0 is the base model weight decay, to ensure the terms all have the same size in norm. In other words, when using decoupled weight decay, the base weight decay term should not scale with model size. See also Dey et al. (2025).

3.2 GROUPED QUERY ATTENTION

Grouped query attention (GQA) reduces computational cost by repeating the key and value heads in the Transformer (Ainslie et al., 2023). In a standard multi-headed attention layer, the key and value projections are given by weights $\mathbf{W}_K \in \mathbb{R}^{n \times n}$ and $\mathbf{W}_V \in \mathbb{R}^{n \times n}$, where n is the embedding dimension. These matrices are partitioned into H heads of size n/H each and the i -th head is computed as $k_i = (\mathbf{W}_K x)_i$, $v_i = (\mathbf{W}_V x)_i$. In GQA, the number of parameters is reduced by using only p distinct key/value heads, where $H/p = r$ denotes the number of repetitions of each key/value head group. We then define matrices $\mathbf{W}_{p,K}, \mathbf{W}_{p,V} \in \mathbb{R}^{\frac{n}{r} \times n}$, and construct the full key and value weights by concatenating along the output dimension

$$\mathbf{W}_K^\oplus = \bigoplus_{m=1}^r \mathbf{W}_{p,K}, \quad \mathbf{W}_V^\oplus = \bigoplus_{m=1}^r \mathbf{W}_{p,V}, \quad (5)$$

where \oplus denotes concatenation along the first dimension³.

Consider the initial weight matrix \mathbf{W}_0 for either the key or value projections, and its concatenation version \mathbf{W}_0^\oplus , and let \mathbf{W}_t and \mathbf{W}_t^\oplus denote their corresponding weight updates. To begin, applying the law of large numbers and the central limit theorem to equation 2, we obtain

$$\|\mathbf{W}_0^\oplus\|_{\mathbb{E}} = \mathbb{E}_x \left[\Theta \left(\frac{\left(\sum_{k=1}^n \left(\sum_{j=1}^n (W_0^\oplus)_{kj} x_j \right)^2 \right)^{\frac{1}{2}}}{\left(\sum_{k=1}^n x_k^2 \right)^{\frac{1}{2}}} \right) \right] = \mathbb{E}_x \left[\Theta \left(\frac{\left(r \sum_{k=1}^{\frac{n}{r}} \left(\sum_{j=1}^n (W_0)_{kj} x_j \right)^2 \right)^{\frac{1}{2}}}{\left(\sum_{k=1}^n x_k^2 \right)^{\frac{1}{2}}} \right) \right].$$

Therefore,

$$\|\mathbf{W}_0^\oplus\|_{\mathbb{E}} = \Theta \left(\frac{\left(r \times \frac{n}{r} \times n \times \sigma^2 \right)^{\frac{1}{2}}}{n^{\frac{1}{2}}} \right) = \Theta \left(\sigma n^{\frac{1}{2}} \right).$$

To satisfy the spectral condition in equation 1, we require $\sigma = \Theta(n^{-1/2})$. Importantly, this corresponds to the expected operator norm for \mathbf{W}^\oplus , not the spectral norm of the constituent matrix \mathbf{W} . Because \mathbf{W}_0 has full rank with probability 1, its spectral norm can be computed directly using Bai-Yin (Bai & Yin, 1993; Yin et al., 1988)

$$\|\mathbf{W}_0\| = \Theta \left(\sigma \left(\sqrt{n} + \frac{\sqrt{n}}{\sqrt{r}} \right) \right) = \Theta \left(\frac{1 + \sqrt{r}}{\sqrt{r}} \right). \quad (6)$$

Moreover, in terms of spectral norms, $\|\mathbf{W}_0^\oplus\| = \sqrt{r} \|\mathbf{W}_0\|$ (Lemma 1), so that the spectral norm and the expected operator norm do not agree in this setting (see Figure 2).

The computation in equation 6 is critical for determining the required learning rate, since we require $\|\Delta \mathbf{W}_t\| = \Theta(\|\mathbf{W}_0\|)$. To this end, we compute η in the usual manner. Assuming the use of the Adam optimizer with update step \hat{r}_t , we have

$$\|\Delta \mathbf{W}_t\| = \eta \|\hat{r}_t\| = \Theta \left(\frac{\eta n}{\sqrt{r}} \right) = \Theta \left(\frac{1 + \sqrt{r}}{\sqrt{r}} \right).$$

From this we easily deduce that $\eta = \Theta \left(\frac{1 + \sqrt{r}}{n} \right)$. We normalize by a factor of two to ensure that when $r = 1$ our scalings agree with the usual full-rank hidden layer scalings:

$$\sigma = \frac{1}{\sqrt{n}} \sigma_0, \quad \eta = \frac{1 + \sqrt{r}}{2n} \eta_0. \quad (7)$$

³Note that concatenation and matrix multiplication commute: if $\mathbf{A} \in \mathbb{R}^{m \times n}$ and $x \in \mathbb{R}^n$, we have $\mathbf{A}^\oplus x = (\mathbf{A}x)^\oplus$, which follows directly by writing the product in its index form.

Through the above derivations, we arrive at the parameterization of Transformers with GQA as summarized in Table 1.

Our GQA- μ P can adapt to any group size by following equation 7. Empirically, we evaluate $r \in \{1, 2, 3, 4, 5, 6, 12\}$. These values cover commonly used settings, including $r = 4$ for Llama-3 8B and Mistral 7B, $r = 8$ for Llama-2/3 70B and Qwen-2.5 72B, and $r = 12$ for Cohere Command R+ (e.g., 96 query heads and 8 key/value heads).

To clarify, our mathematical framework is asymptotically valid with respect to r . However, in practice, r is not scaled to infinity in the same way as the network width n is. Since $n \geq r$, the extreme limit where $r = n$ would force the model to have single-parameter attention heads. Thus, while our asymptotic analysis is sound, this particular infinite limit is not a realistic scenario that would actually be used. The typical range of r in practice usually does not exceed 16, which may not be asymptotically large. However, we would like to emphasize that our primary objective in scaling with r is empirical: to prevent learning-rate drift when changing the number of repetitions r . Our derivations remain valid in the asymptotic limit, which is merely a mathematical consequence of the theory rather than the practical setting we target.

3.3 COMPLETE-P DEPTH SCALING

We now turn to the depth scaling of residual networks. Complete-P (Dey et al., 2025), derives depth scalings by relying on an additional desideratum of “no lazy learning.” We show that we do not need this additional assumption. We demonstrate that applying the standard μ P desideratum to the spectral norm automatically prevents the no lazy learning.” assumption. In this section, we show that applying our framework naturally recovers the exact same scaling as in Complete-P.

Consider the stacked hidden layers, where the output of the ℓ -th layer is given by the residual update:

$$G^\ell(x) = x + \beta g^\ell(x) \quad \text{for } 1 \leq \ell \leq L. \quad (8)$$

Here, $x \in \mathbb{R}^n$ is the input, $g^\ell : \mathbb{R}^n \rightarrow \mathbb{R}^n$ represents the residual branch, and β is a scaling constant independent of the layer index ℓ . To formalize our analysis and address the network dynamics rigorously in the large-width ($n \rightarrow \infty$) and large-depth ($L \rightarrow \infty$) limits, we state the following assumptions explicitly:

- **Assumption 1 (Input Scaling):** The network inputs satisfy $\|x\|_2 = \Theta(\sqrt{n})$. This ensures that the base compositional units satisfy the spectral condition in equation 1.
- **Assumption 2 (Stable Operator Norms):** $\|g^\ell\| = \Theta(1)$, $\|\Delta g^\ell\| = \Theta(1)$, g^ℓ is full-rank, and $\beta \|g^\ell\| < 1$.
- **Assumption 3 (No Exact Cancellation):** This is a standard assumption in the μ P and Tensor Programs literature (Yang & Hu, 2021). For more intuition about this, please refer to A.3.

Let $\bar{G}_t^\ell = \bigcirc_{k=1}^\ell G_t^k$ represent the composition of the first ℓ layers at training step t . We can express the network recursively:

$$\bar{G}_t^\ell = \bar{G}_t^{\ell-1} + \beta g_t^\ell \circ \bar{G}_t^{\ell-1}. \quad (9)$$

Under Assumption 3, taking the norm yields the following asymptotic relation:

$$\|\bar{G}_t^\ell\| = \Theta\left(\|\bar{G}_t^{\ell-1}\| + \beta \|g_t^\ell\| \|\bar{G}_t^{\ell-1}\|\right). \quad (10)$$

Because Assumption 2 dictates $\|g_t^\ell\| = \Theta(1)$, every layer effectively adds a proportional factor of β to the norm estimate. We can formalize the resulting depth-dependent bound via a recursive induction argument. For the base case, at the input, $\|\bar{G}_t^0\| = \|I\| = 1 \leq \Theta(1)$. Assume the bound holds for layer ℓ , such that $\|\bar{G}_t^\ell\| \leq \Theta(1 + \ell\beta)$. For layer $\ell + 1$, we substitute the hypothesis into our asymptotic relation:

$$\|\bar{G}_t^{\ell+1}\| \leq \Theta\left(\|\bar{G}_t^\ell\| + \beta \|\bar{G}_t^\ell\|\right) \leq \Theta((1 + \ell\beta) + \beta(1 + \ell\beta)) = \Theta(1 + \ell\beta + \beta + \ell\beta^2).$$

Because we are analyzing regimes where $\beta < 1$, the higher-order term $\ell\beta^2$ is dominated by the linear terms ($\beta^2 < \beta$). Thus, the expression simplifies to:

$$\left\| \overline{G}_t^{\ell+1} \right\| \leq \Theta(1 + (\ell + 1)\beta).$$

By induction, evaluating this at the final layer yields the total forward pass bound:

$$\left\| \overline{G}_t^L \right\| = \Theta(1 + L\beta). \tag{11}$$

To maintain stable representations and avoid network explosion or vanishing signals, we require the final norm to be independent of depth, i.e., $\Theta(1 + (\ell + 1)\beta) = \Theta(1)$. Setting this equality forces $L\beta = \Theta(1)$, which directly implies that $\beta = \Theta(L^{-1})$.

We single out a minor point of confusion: for a fixed, finite depth network (e.g., $L = 2$), a constant value such as $\beta = 1/2$ naturally satisfies this requirement because $1/2 = O(1/L)$ for that specific L . However, when considering the asymptotic limit where $L \rightarrow \infty$, the parameter β cannot be a static constant larger than $1/L$; it must shrink in exact proportion to the total depth to prevent the $L\beta$ term from diverging. Conversely, choosing a faster shrinking exponent, such as $\beta = \Theta(L^{-\alpha})$ for $\alpha > 1$ (Yang et al., 2023b), causes the residual branches to vanish entirely, degenerating into trivial dynamics. Therefore, $\beta = \Theta(L^{-1})$ guarantees stability without sacrificing expressivity, arriving at the exact same bound as Dey et al. (2025) through an alternate derivation.

4 EMPIRICAL RESULTS

In this section, we present our empirical results. Details of model configurations and experimental setups are provided in Appendix B.1.

Coordinate-Checks Demonstrate the Necessity for Spectral Feature Learning: As discussed in Section 3, validating feature learning by measuring the norms of h^ℓ and Δh_t^ℓ can be misleading. Figures 4 plot $\left\| \Delta h_t^\ell \right\|$ for the vanilla Adam- μ P implementation. The coordinate check would suggest transferable learning rates, yet empirical results show otherwise (see Figure 1, middle). By contrast, when we instead examine the spectral norm conditions in equation 1 (Figure 5), the model fails the coordinate check: a clear non-linear dependence on the number of KV heads of the model, which explains the lack of transferable dynamics.

Coordinate-Checks Demonstrate a Qualitative Dependency on r : Because the vanilla Adam- μ P implementation and our implementation share the same initialization scaling, we do not compare $\left\| W \right\|$ directly. Instead, Figure 5 presents the coordinate checks for the vanilla Adam- μ P implementation, while Figure 6 shows the corresponding coordinate checks for our proposed GQA scaling. Our method passes the coordinate check, thereby enabling μ -transfer of learning rate. By contrast, the vanilla Adam- μ P implementation shows a persistent dependency on the number of KV heads, explaining why the learning rate does not transfer in this case.

Learning Rate Transfer for Grouped Query Attention: We perform an ablation study comparing the standard parameterization, the vanilla Adam- μ P implementation (where the KV heads are initialized as hidden layers), and our proposed GQA- μ P. The results of this ablation study are summarized in Figure 1. We observe that the vanilla Adam- μ P scaling does not account for the shift induced by using GQA, whereas our proposed scaling brings the optimal learning rates into a much narrower region. Noise inherent to GQA training is already evident in these plots and becomes more pronounced as the number of KV heads decreases. This noise is apparent in both the coordinate checks from Figure 6 as well as in Figure 2. We provide an explanation for this phenomenon in the following paragraph.

Expected Variance in GQA Transfer: From the perspective of μ P, the nature of GQA introduces a dichotomy: one may achieve feature learning in the sense of equation 1 and thereby obtain learning rate transfer, but at the cost of increasingly noisy dynamics as the number of KV heads decreases; alternatively, one may constrain the variance as we decrease the number of KV heads to stabilize the training, but this leads to a shift in optimal learning rate. Consequently, we suggest that in scenarios where transferable dynamics are critical, it may be preferable to avoid using GQA altogether.

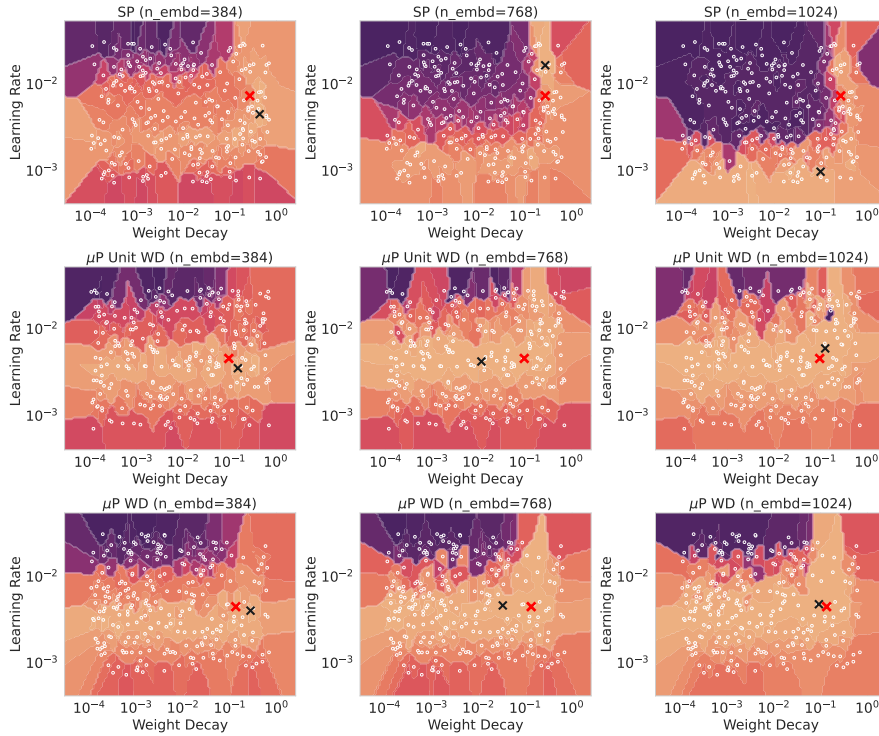


Figure 3: Voronoi interpolation for random sweeps over both learning rate and weight decay. The top row is standard parameterization. The middle row is the vanilla Adam- μ P implementation suggested in Yang et al. (2022). The bottom row is our proposed implementation. Each column corresponds to a different size model, with the number of parameters increasing from left to right. For each model and implementation, we plot the best trial. Hidden dimension, depth, batch size, and training iterations are all scaled. Lighter colors indicate lower loss, darker colors indicate higher loss. The red crosses mark the average (learning rate, weight decay) pair, where each coordinate is averaged over the model sizes, while the black crosses are the optimal pair for each experiment.

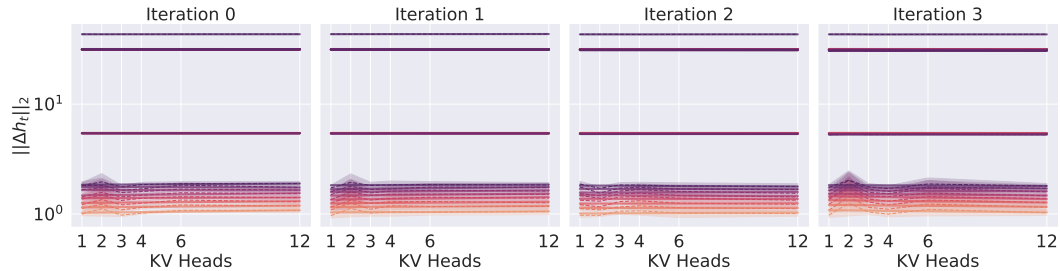


Figure 4: Coordinate checks in the style of Yang et al. (2022) for the activation update norms $\|\Delta h_t^\ell\|_2$ under the vanilla Adam- μ P implementation. Together, these coordinate checks indicate that the implementation is correct, and that feature learning and thus learning rate transfer should occur. However, Figure 1 shows that learning rate transfer for this implementation does not occur.

μ P (Mostly) Decouples Coupled Weight Decay To examine the transferability of optimal learning rate and optimal weight decay across model scales, we do a random grid search over (learning rate, weight decay) pairs at constant initial standard deviation. We plot our results in Figure 3. We note that under the standard parameterization, neither the learning rate nor weight decay transfers, and that the qualitative properties of the Voronoi-interpolated loss landscape change markedly as the model size increases from 26M to 177M non-embedding parameters. By contrast, both the

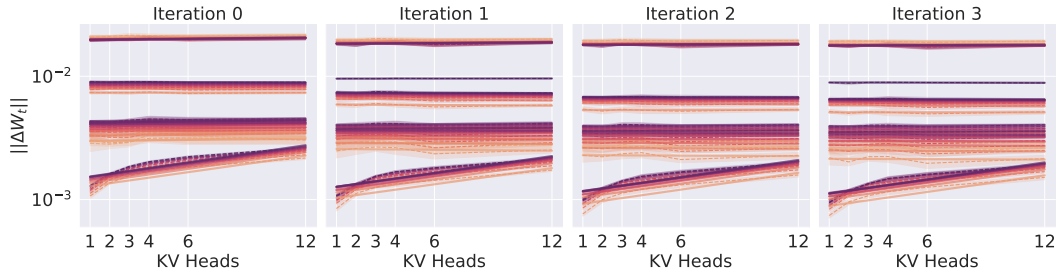


Figure 5: Coordinate checks for $\|\Delta\mathbf{W}\|$ under the vanilla Adam- μP scalings. The model fails the coordinate checks when evaluated using the spectral feature learning condition equation 1. However, as shown in Figure 4, it does pass when evaluated under Yang’s definition of feature learning 3.

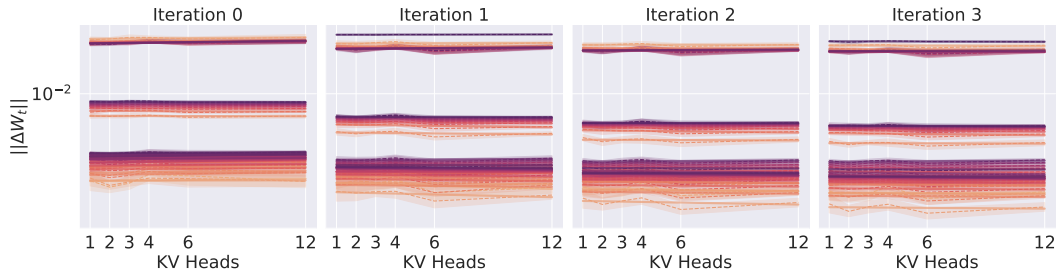


Figure 6: Coordinate checks for $\|\Delta\mathbf{W}\|$ under our proposed GQA scalings. The model has eight hidden layers. Additional experimental details are provided in Appendix B.1.1.

vanilla Adam- μP implementation and our proposed scaling preserve their qualitative properties across model sizes.

For the experiment in Figure 3, we quantify the degree of transfer in Table 6. We find that the variance of both the optimal learning rate and the optimal weight decay across model sizes is lower for our implementation than for the vanilla Adam- μP baseline. Thus, it suggests that our proposed implementation enables the transfer of both learning rate and weight decay across model scales, both qualitatively and quantitatively.

Previous works have argued that the quantity $\tau_{\text{epoch}} = (\lambda_0 \times \eta_0 \times \text{iters})^{-1}$ should transfer instead of weight decay (Wang & Aitchison, 2024; Bergsma et al., 2025). We found that both weight decay and τ_{epoch} transfer in our experimental setting. This is a non-trivial observation since we vary the number of iterations based on the model size. Figure 7 presents the analog of our interpolation diagram. Figure 3 and Table 2 reports the quantitative variance results for τ_{epoch} . We find that τ_{epoch} transfers slightly better than weight decay in our setting.

Table 2: Variance table comparing our implementations across model sizes for the τ_{epoch} experiment from Figure 7.

Implementation	Var. LR	Var. τ_{epoch}	Var. Loss
SP	1.34	2.78	4.87×10^{-1}
μP	4.75×10^{-2}	1.49	4.87×10^{-1}
$\mu\text{P} + \text{WD}$	5.54×10^{-3}	6.56×10^{-1}	4.77×10^{-1}

5 CONCLUSIONS

In this paper, we introduced a novel extension of the spectral μP framework originally developed by Yang et al. (2023a). We can apply our framework to rederive the Complete-P weight decay and depth scalings from Dey et al. (2025). Additionally, we use our framework to derive, for the first time, the μP scalings for grouped query attention (Ainslie et al., 2023). We perform empirical validation in two directions for our work. First, we explore the empirical nature of learning rate transfer for GQA. We find that we can either do noisy learning rate transfer or fail to transfer the learning rate. This dichotomy is a consequence of the competing scalings between the spectral norm and the expected

operator norm. Compared to the standard μP implementation, our method reduces the variance in optimal learning rate during learning rate transfer. Second, we explore the transferability of weight decay across model sizes. We demonstrate that with the standard μP implementation, we can nearly achieve transfer of weight decay. With our implementation, we are able to get much closer to true transfer across both learning rate and weight decay. Future work could extend scaling laws for Mixture-of-Experts or other sparse models.

REFERENCES

- Joshua Ainslie, James Lee-Thorp, Michiel De Jong, Yury Zemlyanskiy, Federico Lebrón, and Sumit Sanghai. Gqa: Training generalized multi-query transformer models from multi-head checkpoints. [arXiv preprint arXiv:2305.13245](#), 2023.
- Maksym Andriushchenko, Francesco D’Angelo, Aditya Varre, and Nicolas Flammarion. Why do we need weight decay in modern deep learning? [arXiv preprint arXiv:2310.04415](#), 2023.
- Zhi-Dong Bai and Yong-Qua Yin. Limit of the smallest eigenvalue of a large dimensional sample covariance matrix. *Ann. Probab.*, 21(3):1275–1294, 1993.
- Shane Bergsma, Nolan Dey, Gurpreet Gosal, Gavia Gray, Daria Soboleva, and Joel Hestness. Power lines: Scaling laws for weight decay and batch size in llm pre-training. [arXiv preprint arXiv:2505.13738](#), 2025.
- Shane Bergsma, Nolan Simran Dey, Gurpreet Gosal, Gavia Gray, Daria Soboleva, and Joel Hestness. Power lines: Scaling laws for weight decay and batch size in LLM pre-training. In [The Thirty-ninth Annual Conference on Neural Information Processing Systems](#), 2026. URL <https://openreview.net/forum?id=bFXbLQzRoZ>.
- Charlie Blake, Douglas Orr, and Carlo Luschi. Unit scaling: Out-of-the-box low-precision training. In [International Conference on Machine Learning](#), pp. 2548–2576. PMLR, 2023.
- Nolan Dey, Gurpreet Gosal, Hemant Khachane, William Marshall, Ribhu Pathria, Marvin Tom, Joel Hestness, et al. Cerebras-gpt: Open compute-optimal language models trained on the cerebras wafer-scale cluster. [arXiv preprint arXiv:2304.03208](#), 2023.
- Nolan Dey, Bin Claire Zhang, Lorenzo Noci, Mufan Li, Blake Bordelon, Shane Bergsma, Cengiz Pehlevan, Boris Hanin, and Joel Hestness. Don’t be lazy: Completep enables compute-efficient deep transformers. [arXiv preprint arXiv:2505.01618](#), 2025.
- Katie Everett, Lechao Xiao, Mitchell Wortsman, Alexander A Alemi, Roman Novak, Peter J Liu, Izzeddin Gur, Jascha Sohl-Dickstein, Leslie Pack Kaelbling, Jaehoon Lee, et al. Scaling exponents across parameterizations and optimizers. [arXiv preprint arXiv:2407.05872](#), 2024.
- Aaron Gokaslan and Vanya Cohen. Openwebtext corpus. <http://Skylion007.github.io/OpenWebTextCorpus>, 2019.
- Aaron Grattafiori, Abhimanyu Dubey, Abhinav Jauhri, Abhinav Pandey, Abhishek Kadian, Ahmad Al-Dahle, Aiesha Letman, Akhil Mathur, Alan Schelten, Alex Vaughan, et al. The llama 3 herd of models. [arXiv preprint arXiv:2407.21783](#), 2024.
- Dan Hendrycks and Kevin Gimpel. Gaussian error linear units (gelus), 2023. URL <https://arxiv.org/abs/1606.08415>.
- Jordan Hoffmann, Sebastian Borgeaud, Arthur Mensch, Elena Buchatskaya, Trevor Cai, Eliza Rutherford, Diego de Las Casas, Lisa Anne Hendricks, Johannes Welbl, Aidan Clark, et al. An empirical analysis of compute-optimal large language model training. [Advances in neural information processing systems](#), 35:30016–30030, 2022.
- Albert Qiaochu Jiang, Alexandre Sablayrolles, Arthur Mensch, Chris Bamford, Devendra Singh Chaplot, Diego de Las Casas, Florian Bressand, Gianna Lengyel, Guillaume Lample, Lucile Saulnier, L lio Renard Lavaud, Marie-Anne Lachaux, Pierre Stock, Teven Le Scao, Thibaut Lavril, Thomas Wang, Timoth e Lacroix, and William El Sayed. Mistral 7b. [ArXiv](#), abs/2310.06825, 2023. URL <https://api.semanticscholar.org/CorpusID:263830494>.

-
- Keller Jordan, Yuchen Jin, Vlado Boza, Jiacheng You, Franz Cesista, Laker Newhouse, and Jeremy Bernstein. Muon: An optimizer for hidden layers in neural networks, 2024. URL <https://kellerjordan.github.io/posts/muon/>.
- Diederik P Kingma and Jimmy Ba. Adam: A method for stochastic optimization. [arXiv preprint arXiv:1412.6980](https://arxiv.org/abs/1412.6980), 2014.
- Zhengzhong Liu, Liping Tang, Linghao Jin, Haonan Li, Nikhil Ranjan, Desai Fan, Shaurya Rohatgi, Richard Fan, Omkar Pangarkar, Huijuan Wang, et al. K2-v2: A 360-open, reasoning-enhanced llm. [arXiv preprint arXiv:2512.06201](https://arxiv.org/abs/2512.06201), 2025.
- Ilya Loshchilov and Frank Hutter. Decoupled weight decay regularization. [arXiv preprint arXiv:1711.05101](https://arxiv.org/abs/1711.05101), 2017.
- Bruno Mlodozienec, Pierre Ablin, Louis Béthune, Dan Busbridge, Michal Klein, Jason Ramapuram, and Marco Cuturi. Completed hyperparameter transfer across modules, width, depth, batch and duration. [arXiv preprint arXiv:2512.22382](https://arxiv.org/abs/2512.22382), 2025.
- Saaketh Narayan, Abhay Gupta, Mansheej Paul, and Davis Blalock. μ nit scaling: Simple and scalable fp8 llm training. [arXiv preprint arXiv:2502.05967](https://arxiv.org/abs/2502.05967), 2025.
- Fabian Schaipp. How to jointly tune learning rate and weight decay for AdamW. <https://fabian-sp.github.io/posts/2024/02/decoupling/>, 2024.
- Xi Wang and Laurence Aitchison. How to set adamw’s weight decay as you scale model and dataset size. [arXiv preprint arXiv:2405.13698](https://arxiv.org/abs/2405.13698), 2024.
- An Yang, Anfeng Li, Baosong Yang, Beichen Zhang, Binyuan Hui, Bo Zheng, Bowen Yu, Chang Gao, Chengen Huang, Chenxu Lv, et al. Qwen3 technical report. [arXiv preprint arXiv:2505.09388](https://arxiv.org/abs/2505.09388), 2025.
- Greg Yang. Wide feedforward or recurrent neural networks of any architecture are gaussian processes. *Advances in Neural Information Processing Systems*, 32, 2019.
- Greg Yang. Tensor programs ii: Neural tangent kernel for any architecture. [arXiv preprint arXiv:2006.14548](https://arxiv.org/abs/2006.14548), 2020a.
- Greg Yang. Tensor programs iii: Neural matrix laws. [arXiv preprint arXiv:2009.10685](https://arxiv.org/abs/2009.10685), 2020b.
- Greg Yang and Edward J Hu. Tensor programs iv: Feature learning in infinite-width neural networks. In *International Conference on Machine Learning*, pp. 11727–11737. PMLR, 2021.
- Greg Yang, Edward J Hu, Igor Babuschkin, Szymon Sidor, Xiaodong Liu, David Farhi, Nick Ryder, Jakub Pachocki, Weizhu Chen, and Jianfeng Gao. Tensor programs v: Tuning large neural networks via zero-shot hyperparameter transfer. [arXiv preprint arXiv:2203.03466](https://arxiv.org/abs/2203.03466), 2022.
- Greg Yang, James B Simon, and Jeremy Bernstein. A spectral condition for feature learning. [arXiv preprint arXiv:2310.17813](https://arxiv.org/abs/2310.17813), 2023a.
- Greg Yang, Dingli Yu, Chen Zhu, and Soufiane Hayou. Tensor programs vi: Feature learning in infinite-depth neural networks. [arXiv preprint arXiv:2310.02244](https://arxiv.org/abs/2310.02244), 2023b.
- Yong-Qua Yin, Zhi-Dong Bai, and Pathak R Krishnaiah. On the limit of the largest eigenvalue of the large dimensional sample covariance matrix. *Probability theory and related fields*, 78:509–521, 1988.
- Chenyu Zheng, Rongzhen Wang, Xinyu Zhang, and Li Chongxuan. Spectral condition for μ p under width-depth scaling. [arXiv preprint arXiv:2603.00541v2](https://arxiv.org/abs/2603.00541v2), 2026.

A ADDITIONAL MATHEMATICAL DETAILS

A.1 DERIVATION FOR ADAM

We demonstrate the applicability of our framework by re-deriving the μ P scalings for Adam. Recall that the Adam optimizer Kingma & Ba (2014) uses hyperparameters β_1 , β_2 , ε , and η and has its optimization steps given by the following components:

$$\begin{aligned} g_t &= \nabla_{\mathbf{W}} f(\mathbf{W}_{t-1}), \\ m_t &= \beta_1 m_{t-1} + (1 - \beta_1) g_t, & v_t &= \beta_2 v_{t-1} + (1 - \beta_2) g_t^2, \\ \hat{m}_t &= \frac{m_t}{1 - \beta_1^t}, & \hat{v}_t &= \frac{v_t}{1 - \beta_2^t}, \end{aligned}$$

with the weight update

$$\mathbf{W}_t = \mathbf{W}_{t-1} - \eta \frac{\hat{m}_t}{\sqrt{\hat{v}_t + \varepsilon}}. \quad (12)$$

The key observation is that the term

$$\hat{\mathbf{r}}_t := \frac{\hat{m}_t}{\sqrt{\hat{v}_t + \varepsilon}} \quad (13)$$

will always have typical size 1 (for ε sufficiently small), and as such the spectral norm can be estimated using the Bai-Yin theorem (Yin et al., 1988; Bai & Yin, 1993), depending on whether the layer is vector-like or matrix-like. Thus, we have the following reasoning. For an input layer, we have

$$\|\Delta \mathbf{W}_t^0\| = \underbrace{\Theta(\eta^0 \sqrt{n})}_{\text{Bai-Yin}} = \underbrace{\Theta(\sqrt{n})}_{\text{equation 1}},$$

which implies that we must choose $\eta^0 = \Theta(1)$. Next, for the hidden layers, we have

$$\|\Delta \mathbf{W}_t^\ell\| = \underbrace{\Theta(\eta^\ell n)}_{\text{Bai-Yin}} = \underbrace{\Theta(1)}_{\text{equation 1}},$$

which leads us to choose $\eta^\ell = \Theta(n^{-1})$. Finally, for the output layer, we have

$$\|\Delta \mathbf{W}_t^{L+1}\| = \underbrace{\Theta(\eta^{L+1} \sqrt{n})}_{\text{Bai-Yin}} = \underbrace{\Theta(n^{-1/2})}_{\text{equation 1}},$$

which leads us to choose $\eta^{L+1} = \Theta(n^{-1})$. There is a subtle nuance in our derivation that is also often overlooked in the literature. We have assumed that the Adam optimizer step is independent of the network width n , but this is not quite true. To see why, consider setting $\beta_1 = \beta_2 = 1$, so that the Adam optimizer step is given simply by

$$\hat{\mathbf{r}}_t = \frac{g_t}{|g_t| + \varepsilon},$$

where g_t is the gradient. For concreteness, consider a hidden layer. Yang et al. (2022) show that the gradient will scale like $\Theta(1/n)$. Thus letting $\bar{g}_t = g_t/n$ be the size 1 normalized gradient updates, we have that the

$$\hat{\mathbf{r}}_t = \frac{\bar{g}_t}{|\bar{g}_t| + n\varepsilon},$$

which is not actually $\Theta(1)$ in n , since for $n = \Omega(\varepsilon^{-1})$, the Adam updates decay like n^{-1} . Thus, to be pedantic and ensure actual feature learning, we must scale $\varepsilon = \varepsilon_0/n$ to continue to achieve feature learning. In practice, we find that this subtlety can be avoided by setting $\varepsilon = 10^{-12}$ instead of the usual default of 10^{-8} ; however, for a complete treatment, this scaling must be included. We note that Dey et al. (2023), Everett et al. (2024) make the same conclusion about scaling the Adam ε parameter and perform an empirical study on its transferability.

A.2 ADDITIONAL DETAILS FOR GROUPED QUERY ATTENTION

Lemma 1. *Scaling Concatenated Spectral Norms.* Let $A \in \mathbf{R}^{n \times \frac{n}{r}}$ for some integer $r \geq 1$, where r is the number of repetitions of key and value heads, be a matrix with spectral norm $\|A\| > 0$. Then letting $A^\oplus := \bigoplus_{j=1}^r A$ we have

$$\|A^\oplus\| = \sqrt{r} \|A\|. \quad (14)$$

Proof of Lemma 1. We denote the r -times concatenation by

$$A^* = \underbrace{[A \ A \ \cdots \ A]}_{r \text{ times}}. \quad (15)$$

Each matrix A has a singular value decomposition $U\Sigma V^T$ for U, V unitary with $U \in \mathbb{R}^{n \times n}$, $V \in \mathbb{R}^{\frac{n}{r} \times \frac{n}{r}}$, and $\Sigma = \begin{bmatrix} \Lambda \\ 0 \end{bmatrix} \in \mathbb{R}^{n \times \frac{n}{r}}$ with Λ a diagonal $\mathbb{R}^{\frac{n}{r} \times \frac{n}{r}}$ matrix. Substituting the SVD into equation 15 we can factor out the unitary matrix U and arrive at

$$A^* = U \begin{bmatrix} \Sigma V^T & \Sigma V^T & \cdots & \Sigma V^T \end{bmatrix} = U \begin{bmatrix} \Lambda V^T & \Lambda V^T & \cdots & \Lambda V^T \\ 0 & 0 & \cdots & 0 \\ \vdots & \vdots & \ddots & \vdots \\ 0 & 0 & \cdots & 0 \end{bmatrix}$$

It remains to find the singular values of this matrix, which give us the spectral norm scaling. To this end, observe that by the unitary of V we have

$$U \begin{bmatrix} \Lambda V^T & \Lambda V^T & \cdots & \Lambda V^T \\ 0 & 0 & \cdots & 0 \\ \vdots & \vdots & \ddots & \vdots \\ 0 & 0 & \cdots & 0 \end{bmatrix} \begin{bmatrix} V\Lambda & 0 & \cdots & 0 \\ V\Lambda & 0 & \cdots & 0 \\ \vdots & \vdots & \ddots & \vdots \\ V\Lambda & 0 & \cdots & 0 \end{bmatrix} U^T = U \begin{bmatrix} r\Lambda^2 & 0 & \cdots & 0 \\ 0 & 0 & \cdots & 0 \\ \vdots & \vdots & \ddots & \vdots \\ 0 & 0 & \cdots & 0 \end{bmatrix} U^T$$

Thus, the largest eigenvalue of AA^T is given by $r\lambda_{\max}^2$, with λ_{\max} being the largest eigenvalue of A , and the desired spectral norm scaling is immediate. \square

Lemma 2. *Let $A \in \mathbf{R}^{n \times n}$ have i.i.d. entries. Then the for $x \sim \mathcal{N}(0, 1)$ with i.i.d. entries, we have that*

$$\|Ax\|_{\mathbb{E}} = \Theta(\|A\|).$$

Proof of Lemma 2. First, note that $\|A\| = \Theta(\sigma\sqrt{n})$, where σ is the variance of the i.i.d. entries of A . Next, observe that we can use the law of large numbers and the central limit theorem to estimate

$$\mathbb{E} \|Ax\|_2^2 = \mathbb{E} \sum_i \left(\sum_j A_{ij} x_j \right)^2 = \Theta(\sigma^2 n^2),$$

and the result follows since $\|x\|_2 = \Theta(\sqrt{n})$. \square

A.3 INTUITION BEHIND NO EXACT CANCELLATION

The intuition is that, in high-dimensional spaces, independently initialized weight matrices and their gradient updates typically act on inputs in weakly correlated, nearly orthogonal directions. Therefore, when we add two such high-dimensional operators, such as W_{t-1} and ΔW_{t-1} , their geometries are unlikely to align in a way that causes significant cancellation. As a result, the norm of the sum remains on the same order as the combined contribution of the two terms, rather than becoming artificially small.

Table 3: Model configurations for the coordinate check experiments from Figures 4, 5, 6.

Width	Depth	Num Heads	Head Size	KV Heads	KV Reps
576	8	12	64	1	12
576	8	12	64	2	6
576	8	12	64	3	4
576	8	12	64	4	3
576	8	12	64	6	2
576	8	12	64	12	1

This assumption captures a basic stability property of high-dimensional neural networks: when an update is added to a weight matrix, the update and the existing weights should not systematically point in opposite directions. If they did, the update could cancel the weights, causing the activations or backpropagated gradients to shrink across layers or training steps. In the extreme case, repeated cancellation would drive internal signals toward zero, preventing the network from learning useful features from the data.

B EXPERIMENTAL DETAILS

B.1 MODEL CONFIGURATIONS

In our experiments, we train Transformer language models with untied embeddings and GELU Hendrycks & Gimpel (2023) nonlinearity. The batch size is chosen using a data-driven optimal batch size in equation 16 based on the total number of training tokens n_{tokens} , where the corresponding sequence length is 8192.

$$B = 0.000733 \times \sqrt{n_{tokens}}. \quad (16)$$

Equation 16 follows the isoloss sweep methodology of Bergsma et al. (2026) but uses a rounded exponent for tractability. Specifically, Bergsma et al. (2026) estimates a scaling exponent of 0.46 and recommends rounding to 0.5. Since we ran independent sweeps on our own data, equation 16 is specific to our setup but aligns structurally with Bergsma et al. (2026).

We use a cosine learning rate schedule with warmup. The number of warmup steps follows equation 17, Dey et al. (2025):

$$n_{warmup} = \min(\text{int}(0.02 * n_{training}), \text{int}(375e6/(B * L))), \quad (17)$$

where B is batch size and L is sequence length.

All of our experiments are conducted using the openwebtext dataset (Gokaslan & Cohen, 2019).

B.1.1 COORDINATE CHECKS

For the coordinate checking we verify that our norms remain stable as we vary the number of kv heads. The specific configurations which we used during the coordinate checks are contained in Table 3. We use weight decay 0 in our coordinate checking experiments, and do all of the computation in `float32`. We used a fixed Adam ϵ of 10^{-12} and an initial standard deviation of 0.02. Other optimizer settings are set to the defaults of PyTorch’s Adam implementation. We perform our experiments on seeds 1 through 10 and plot the average and confidence interval. We use a batch size of 1 and a sequence length of 1024 to ensure quick computation.

B.1.2 GQA ABLATION EXPERIMENT

We train our GQA ablation models to 10 TPP. The configurations used for this experiment can be found in Table 4. We set the base weight decay to be $\lambda_0 = 0.1$. We use a base Adam ε of $10^{-9}/n$, where n is the embedding dimension, to match the predicted Adam ε scaling of Dey et al. (2025). We take three runs for each data point, using seeds 42, 43, 44 for reproducibility.

Table 4: Model configurations for the GQA transfer experiments from Figure 1.

	Params	Non-Emb Params	Width	Depth	Num Heads	Head Size	KV Heads	KV Reps	TPP	Dataset Size (Tokens)	Dataset Size (Sequences)	Batch Size (Tokens)	Batch Size (Sequences)	Iterations
kvr_t.1	125.55	80.62	768	7	12	64	1	12	10	806200000	98413	262144	32	3075
kvr_t.2	126.23	81.31	768	7	12	64	2	6	10	813100000	99255	262144	32	3102
kvr_t.3	126.92	82	768	7	12	64	3	4	10	820000000	100098	262144	32	3128
kvr_t.4	127.61	82.69	768	7	12	64	4	3	10	826900000	100940	262144	32	3154
kvr_t.6	128.99	84.06	768	7	12	64	6	2	10	840600000	102612	262144	32	3207
kvr_t.12	133.12	88.19	768	7	12	64	12	1	10	881900000	107654	270336	33	3262

B.1.3 WEIGHT DECAY TRANSFER EXPERIMENT

Due to the high number of sampling points we only trained our models in the weight decay experiments to 3 TPP, well below the compute optimal horizon (Hoffmann et al., 2022). The configurations used for this experiment can be found in Table 5. We uniformly sample the grid in $\log - \log$ space. We were only able to run one trial per data point, but the high number of trials increase confidence. We sample 250 points on the grid for each implementation and model size.

Table 5: Model configurations for the Weight decay experiments from Figures 3 and 7.

	Params	Non-Emb Params	Width	Depth	Num Heads	Head Size	KV Heads	KV Reps	TPP	Dataset Size (Tokens)	Dataset Size (Sequences)	Batch Size (Tokens)	Batch Size (Sequences)	Iters.
jwd-small	48.82	26.38	384	4	6	64	6	1	3	79140000	9661	81920	10	966
jwd-medium	125.96	81.07	768	6	12	64	12	1	3	243210000	29689	147456	18	1649
jwd-large	237.17	177.31	1024	10	16	64	16	1	3	531930000	64933	212992	26	2497

B.2 FAILURE OF YANG-TYPE COORDINATE CHECKING

Yang et al. (2022) suggest measuring $\|h_t\|_2$ and $\|\Delta h_t\|_2$ to verify that a μP implementation is correct by comparing these norms during training to feature learning conditions in equation 3. In Figure 4 we plot $\|\Delta h_t\|_2$ for the vanilla Adam- μP implementation while varying only the number of kv heads. Note that the the implementation passes a coordinate check, but as discussed theoretically in Section 3, and empirically in Section 4 the learning rate does not transfer for this implementation (see Figure 1).

Coordinate checks on our proposed spectral condition from equation 1, however, capture the failure of feature learning (see Figure 5).

B.3 TRANSFER AT COMPUTE-OPTIMAL TRAINING HORIZONS

To check that the behaviour observed at 10 TPP persists at more realistic training lengths, we repeat the learning-rate sweep at 20 TPP, scaling from a 136M proxy model to a 1.2B target model across $r \in \{1, 2, 4, 8\}$. Figure 8 reports the results on a half-power LR grid for the 136M proxy and whole-power steps for the 1.2B target. The 1.2B target optimum lands at 2^{-9} under both parameterizations, so the transfer question reduces to whether the 136M proxy identifies the same learning rate. Under vanilla μP , three of the four 136M proxy optima $r \in \{1, 2, 4\}$ drift to $2^{-8.5}$, half a power above the 1.2B target, while only $r=8$ recovers 2^{-9} . Under GQA- μP , two of the four proxy optima $r \in \{4, 8\}$ coincide with the target at 2^{-9} , and the remaining two $r \in \{1, 2\}$ sit at $2^{-8.5}$. GQA- μP therefore reduces but does not eliminate the residual r -dependence at this horizon. Combined with the coordinate-check result in Figure 6, this still favours GQA- μP as the theoretically correct choice, particularly at shorter training horizons where the bias under vanilla μP is larger as shown in Figure 1.

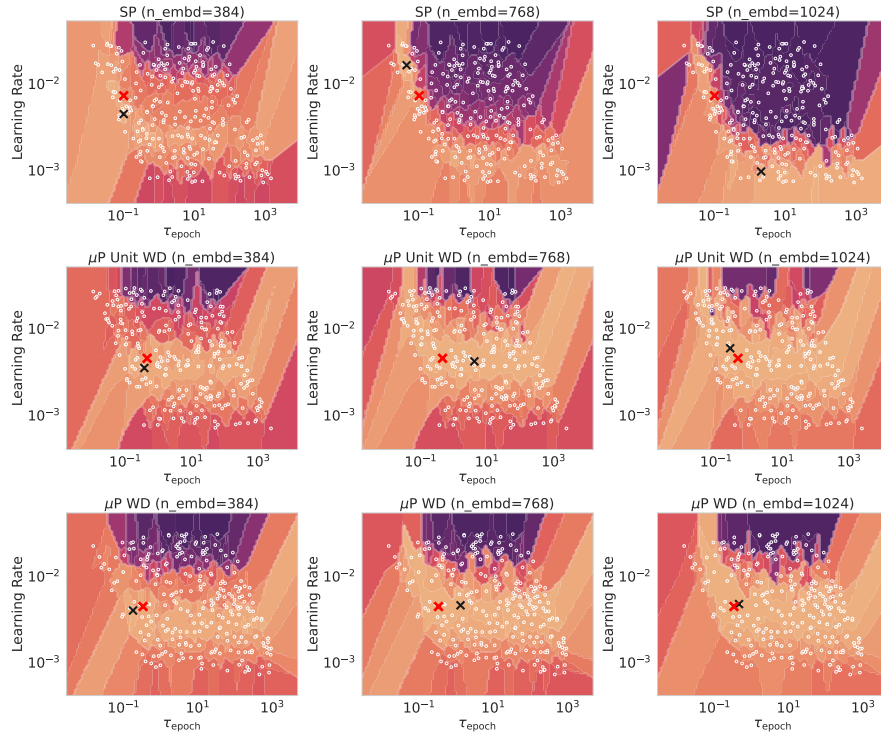


Figure 7: Voronoi interpolation for random sweeps over both learning rate and τ_{epoch} Wang & Aitchison (2024). The top row is standard parameterization. The middle row is the vanilla Adam- μP implementation suggested in Yang et al. (2022). The bottom row is our proposed implementation. Each column is a different size model, increasing in number of parameters from left to right. For each model and implementation we plot the best trial. We scale the hidden dimension, depth, batch size, and training iterations. Lighter colors are lower loss, darker colors are higher loss. The red x is the average (learning rate, weight decay) pair, where each coordinate is averaged over the model sizes, while the black x is the optimal pair for each experiment.

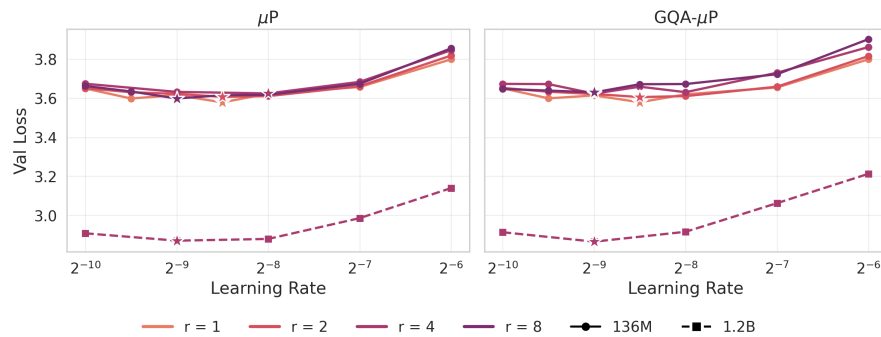


Figure 8: Learning-rate transfer at 20 tokens-per-parameter (TPP) under vanilla Adam- μP (left) and GQA- μP (right). The 136M proxy is swept at $r \in \{1, 2, 4, 8\}$ on a half-power LR grid and the 1.2B target is swept at $r=4$ on whole-power steps. Colour encodes r and linestyle encodes model size; stars mark the optimal learning rate for each configuration. The 1.2B target optimum lands at 2^{-9} under both parameterizations. Under vanilla μP the 136M proxy optima drift to $2^{-8.5}$ for three of the four r values, whereas under GQA- μP two of the four proxy optima coincide with the target at 2^{-9} ; the residual r -dependence is smaller but not fully eliminated at this training horizon.

Table 6: Variance table comparing our implementations across model sizes for the weight decay experiment from Figure 3.

Implementation	Var. LR	Var. WD	Var. Loss
SP	1.34	3.83×10^{-1}	4.87×10^{-1}
μ P	4.75×10^{-2}	1.38	4.87×10^{-1}
μ P + WD	5.54×10^{-3}	7.51×10^{-1}	4.77×10^{-1}

B.4 MORE RESULTS ABOUT WEIGHT DECAY

We used the same data that was collected from Figure 3 to analyze whether or not our experimental testbed demonstrates transfer over τ_{epoch} , as is suggested by (Wang & Aitchison, 2024; Bergsma et al., 2025; Dey et al., 2025). We find that we get slightly better transfer in τ_{epoch} than we do with weight decay, using the same data. We plot the variance in our optimal configurations in Table 2. Like for the case of weight decay transfer (see Figure 3), we find that our suggested implementation outperforms both the standard parameterization and the vanilla Adam- μ P implementation from Yang et al. (2022).

C LLM STATEMENT

We did not use LLMs in a significant way to aid our research during the completion of this work. Our LLM usage did not extend beyond using code assistants like copilot and for polishing the writing in our manuscript.